

Master Thesis

Master's Programme in Embedded and Intelligent Systems, 120 credits



Analyzing white blood cells using deep learning techniques

Computer science and engineering, 30 credits

Halmstad 2020-10-15

Suraj Neelakantan, Sai Sushanth Varma Kalidindi



Suraj Neelakantan and Sai Sushanth Varma Kalidindi: *Analyzing white blood cells in blood samples using deep learning techniques*, ,

© December 2019 - September 2020

SUPERVISORS:

Mattias Ohlsson

LOCATION:

Halmstad

TIME FRAME:

December 2019 - September 2020

ABSTRACT

The field of hematology involves the analysis of blood and its components like platelets, red blood cells, white blood cells. The outcome of this analysis can be vital in determining the condition of the human body and it is important to obtain accurate results.

A deep learning algorithm scans over the given input data for unique features and learns them. Then it identifies these features and correlates them to give the result. This can save a significant amount of time and manual work. In contrast, a traditional machine learning algorithm requires the developer to carry-out the feature engineering.

This thesis involves the analysis of white blood cells (WBC) using deep learning techniques. In collaboration with a hematology company HemoCue AB based in Angelholm, we will be developing deep learning algorithms for the analysis of white blood cells in the HemoCue® WBC DIFF System.

Predominantly, there are two stages in this thesis. The first stage is white blood cell identification, which is used to calculate the number of white blood cells in the given blood sample. The next stage is to identify the different types of white blood cells with which the concentration of each type of WBC in the given blood sample is calculated. We have explored different classification approaches like 'one vs all' and '4-class classifier', and have developed two CNN architectural designs i.e. 'multi-input' and 'multi-channel'. On comparing the performance of all these design approaches, a final integrated model is put forth for the analysis of WBCs in the company's device.

The proposed 'one vs all' classification approach combined with a 3-class CNN classifier has yielded very promising results with a combined accuracy 95.45% in WBC identification and 90.49% in WBC differential classification.

Dedicated to all the lives lost due to COVID-19

ACKNOWLEDGEMENTS

First, we would like to pay our sincere and special regards to our supervisor Mattias Ohlsson (Professor, Halmstad University), for his constant support and guidance towards the right direction.

We would like to express our deepest gratitude to HemoCue AB based in Angeholm and Tomas Jonasson Bjarang (System Developer, HemoCue AB) offering deep insights on hematology and analysis of white blood cells. On a personal note, it is very exciting to get to know about the company and their research.

We are indebted to our examiner Slawomir Nowaczyck, whose constructive feedback at every stage helped us to shape our thesis in a better way.

Last but not the least, we would like to thank our family, friends and The Almighty.

CONTENTS

1	INTRODUCTION	6
1.1	White blood cells	6
1.2	Clinical Significance of WBC Analysis	6
1.3	HemoCue AB and HemoCue®WBC DIFF System	7
1.4	Convolutional neural network	8
1.5	Aim of thesis	8
1.6	Approaches	9
1.7	Thesis disposition	9
2	BACKGROUND	10
2.1	Related Works	10
2.1.1	Feature Extraction	10
2.1.2	K-means clustering with Convolutional Neural Network	10
2.1.3	One vs All classification	11
2.1.4	Multi-channel neural networks	11
2.1.5	Multi-input neural networks	11
2.2	Novelty	11
3	METHODOLOGY	13
3.1	Preface	13
3.2	Data Collection	15
3.2.1	Training and Validation split	16
3.3	Pre-Processing	18
3.4	Design	19
3.4.1	WBC identification	19
3.4.2	WBC differential classification	21
3.5	Architecture	24
3.5.1	Convolutional neural network	24
3.5.2	Proposed CNN architectural approaches	25
3.5.3	Multi-channel convolutional neural network classification	26
3.5.4	Multi-input convolutional neural network classification	26
3.6	Final integrated design	27
3.7	Assessment Method	29
3.8	Hardware	30
3.8.1	Laptop	30
3.8.2	Computational server	30
4	RESULTS AND ANALYSIS	31
4.1	Analysis	31
4.1.1	Loss and Accuracy curves	31
4.1.2	Hyper-parameter selection	31
4.2	Results	32

4.2.1	Accuracy	32
4.2.2	Confusion Matrix	33
4.2.3	Verification plot	36
5	DISCUSSION	38
5.1	Interpretation	38
5.1.1	OVA and 3-class classifier	38
5.1.2	Multi-channel and Multi-input architectural design approaches	39
5.1.3	Basophil concentration	39
5.2	Limitations	40
6	CONCLUSION AND FUTURE WORKS	41
6.1	Conclusion	41
6.2	Future Works	41
A	DECLARATION	46

LIST OF FIGURES

Figure 1	Analysis of WBC differential concentration on smoking individuals. 7	
Figure 2	HemoCue®WBC DIFF System (<i>source:HemoCue AB</i>). 8	
Figure 3	Image of a stained blood smear with a WBC 13	
Figure 4	Flow diagram of WBC image processing inside HemoCue®WBC DIFF System. 14	
Figure 5	The above image represents a set of stacked images with different focal lengths building up to the image representation of the given blood sample. The small dots in the images are WBCs, exemplified by the five smaller (zoomed in) images in the bottom row. 14	
Figure 6	For each found WBC in the blood sample a bounding box is created. The smaller images within the bounding box forms the stack of 37 images for this WBC. Within that stack, the best-focused image plane is identified. 15	
Figure 7	Single blood cell. 17	
Figure 8	Double blood cell. 17	
Figure 9	Triple blood cell. 17	
Figure 10	Trash. 17	
Figure 11	Neutrophil. 17	
Figure 12	Eosinophil. 17	
Figure 13	Lymphocyte. 17	
Figure 14	Mono-cyte. 17	
Figure 15	Training data for WBC identification. 18	
Figure 16	Training data for WBC classification. 18	
Figure 17	Cell identification data after image augmentation. 19	
Figure 18	Cell differential data after image augmentation. 19	
Figure 19	Model flow diagram of 4-class WBC classification. 20	
Figure 20	Model flow diagram of OVA and 3-class WBC classification. 21	
Figure 21	Plot of initial total WBC count vs corrected WBC count. 22	
Figure 22	Model flow diagram for 4-class WBC differential classification. 22	

Figure 23	Model flow diagram of OVA and 3-class WBC differential classification. 23	
Figure 24	Visualization of an example CNN architecture. 24	
Figure 25	Before and After using dropout. 25	
Figure 26	Image before the focused plane. 26	
Figure 27	Plane 1 image in the image stack. 26	
Figure 28	Image after the focused plane. 26	
Figure 29	Multi-channel convolutional neural network for cell identification. 27	
Figure 30	Multi-input convolutional neural network for cell identification. 28	
Figure 31	Integrated model flow diagram. 28	
Figure 32	Accuracy and Loss curves of 3-class differential model. 31	
Figure 33	Example of a confusion matrix from our final model OVA 4-class CNN classifier. 33	
Figure 34	Verification plot of OVA and 3-class classifier. 37	

LIST OF TABLES

Table 1	Description of the data received.	16
Table 2	List of set hyper-parameters for the OVA and 3-class classification model.	32
Table 3	Classification results for different methods in WBC identification part.	33
Table 4	Classification results for different methods in WBC Differential part.	33
Table 5	Results from confusion matrices of different design methods in WBC identification.	34
Table 6	Results from confusion matrices of different design methods in WBC differential classification.	34
Table 7	Performance metrics for different methods in cell identification	35
Table 8	Performance metrics for different methods in cell differentiation	36
Table 9	Weighted-average performance metrics for different methods	36

INTRODUCTION

This chapter opens with the motivation to the research. Following sections gives a brief introduction to the white blood cells(WBC) importance analysis of WBC and aim of the thesis with the approaches used to achieve this aim.

1.1 WHITE BLOOD CELLS

Blood and its components play a vital role in the proper functioning of the human body. The components of the blood can be broadly classified into erythrocytes (red blood cells), platelets and leukocytes (white blood cells). Of the three, WBCs are the primary component which is involved in the body's immune response and account for about 1 percent of the blood.

White blood cells are produced in the bone marrow and are present in blood and lymph tissues. They are further categorized into five groups: basophil, eosinophil, lymphocyte, monocyte, and neutrophil. Each type of WBC has its own significance. Monocytes, breaks down any bacteria that enters the body and tend live longer than the rest of WBCs. Lymphocytes, creates antibodies to fight against viruses like COVID-19, bacteria or any other harmful invader to the human body. Neutrophils are in larger number and are generally the first line of defence in the human body. They kill and digest bacteria and fungi. Eosinophils fights allergies, carcinogens and parasites. The last type, Basophils are minute and less in number.

1.2 CLINICAL SIGNIFICANCE OF WBC ANALYSIS

The normal total count of WBC in a person is 4500 - 11000 per micro litre of blood[23]. Variations in the count of WBCs and the concentration of different WBCs are analysed to determine the presence of an infection. There are many factors which are responsible for variations in the WBC count. For example, the study conducted by Pedersen et.al [4] shows that there is an increase in white blood cells among smoker as shown in figure 1.

The HemoCue®WBC DIFF System is primarily used to detect these variations in WBC count and differential concentration. Conditions like 'leukopenia' where there is a decrease in total count of WBC[23] can be diagnosed by observing the variation in total WBC count.

In recent times, the outbreak of COVID-19 has created shock waves all over the world. Immunity plays an important role in fighting

104 607 individuals from the Copenhagen General Population Study

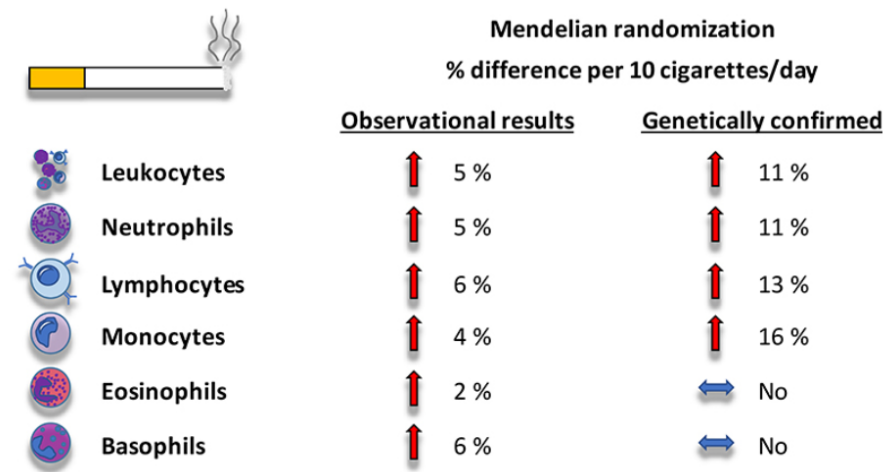


Figure 1: Analysis of WBC differential concentration on smoking individuals.

this deadly virus. Some clinical characteristics of COVID-19 involve white blood cells. According to the studies conducted by Huang et al.[24][27], W. Guan et al.[25], and Qin C et al.[26] that a low lymphocyte count is common and in some cases severe. Low lymphocyte count also impacts the neutrophil to lymphocyte ratio with increased neutrophil percentage as a marker to observe.

With the analysis of WBC having so much importance taking into account the severity of COVID-19, the need of giving the accurate results of total WBC concentration and the differential count is high. With the recent developments in machine learning, such as deep neural networks, we are optimistic to improve the accuracy of the WBC analysis.

1.3 HEMOCUE AB AND HEMOCUE[®] WBC DIFF SYSTEM

This project is carried out in collaboration with a company, HemoCue AB. HemoCue AB is a global leader in the field of point-of-care testing. 'It must be possible'- conviction of HemoCue has been their driving force [1], and this has been a great motivational statement for us.

HemoCue[®]WBC DIFF System, shown in figure 2 is a device used to measure the total white blood count with a 5-part differential in minutes. The system works in the following way: A droplet of blood is drawn into a microcuvette which is inserted into the device. The HemoCue[®]WBC DIFF System gives the total count of WBC and the differential count in minutes after the cuvette is inserted into the instrument[2]. The thesis is carried out using the data from the



Figure 2: HemoCue® WBC DIFF System (source: HemoCue AB).

HemoCue® WBC DIFF System using new techniques to enhance the performance the device.

1.4 CONVOLUTIONAL NEURAL NETWORK

Convolutional neural networks are inspired by the neural networks in the human body and have been one of the most influential innovations in the field of computer science. When we see a dog and a cat, we interpret different features like paws, face and so on to differentiate between the two animals. This interpretation is done with the help of our biological neural networks. In a similar way, the computer is able to perform this classification with the help of a convolutional neural network.

When the input is given to a convolutional neural network, it identifies low level features like edges and curves and when the input passes through its series of layers, and builds an abstract knowledge of unique features in the input. This is just an overview of the convolutional neural networks. More specifics about the convolutional neural networks are discussed in the coming sections.

1.5 AIM OF THESIS

The main intention of this thesis is to develop an algorithm using deep learning techniques for the HemoCue® WBC DIFF System shown in figure 2, manufactured by HemoCue AB.

The instrument currently uses a more traditional machine learning approach for the WBC analysis. We aim to develop new meth-

ods based on newer techniques that have emerged during the recent years.

1.6 APPROACHES

In this thesis, we intend to use deep learning techniques for the classification of four different types of WBC (Lymphocytes, Monocytes, Neutrophils, and Eosinophils) and the total count of WBC in a sample.

There are different approaches that can be followed in field deep learning, depending on the data and requirements. We are presenting two different WBC classificational approaches namely, a multi-class classification and one-vs-all classification. Also, we will present two approaches at the architectural level of CNNs namely, multi-channel CNN classification and multi-input CNN classification.

Our intent is to build a model using deep learning techniques and to avoid in the manual computation of features. Also, use the depth of the image stack by using different image planes and make the algorithm more robust.

1.7 THESIS DISPOSITION

Chapter 1 gives a short motivation to the research area. It also gives an introduction stating the aim of the thesis and the different techniques used.

Chapter 2 discusses about the techniques used in WBC analysis and also different approaches that can employed in convolutional neural networks.

Chapter 3 describes the methods used in the analysis of WBC and the design of convolutional neural network used in the thesis.

Chapter 4 showcases the results of the thesis and comparison of the results from different techniques used in the thesis.

Chapter 5 discusses what each result shown in the above section mean and also the possible limitation in the thesis.

Chapter 6 a conclusion to the thesis and also possible works that can be done in the future.

BACKGROUND

This chapter provides background information for understanding our thesis. We discuss couple of articles related to WBC analysis using machine learning and also we discuss articles on different approaches in CNN architecture which can be used for WBC analysis.

2.1 RELATED WORKS

2.1.1 *Feature Extraction*

Here is an example of how manual feature engineering is carried out in WBC analysis. In the paper, Elen et al. 2019 [6] have used statistical and geometrical information extracted from the images used as input for the algorithm. A feature vector consisting of 21 statistical features was extracted by calculating histogram values for each color band in the input image and 14 geometrical features were extracted by computing the area, perimeter, radius, and other parameters by converting the input image into grayscale first. Thus, a combined feature vector consisting of 35 features was used for the classification algorithm.

The authors have discussed the properties of many machine learning algorithms that can be used for WBC classification. The paper emphasizes feature extraction for WBC classification and showcases the performance of different classification algorithms using the extracted feature set.

2.1.2 *K-means clustering with Convolutional Neural Network*

Segmentation can be explained as the process of dividing the image into different groups of pixels. The purpose is to simplify the image and segmentation of white blood cells in blood smear is a difficult task because of its non-uniform color and disparities. Hence, K-means clustering is used for segmentation. Authors Su M.C, Cheng C.Y et al in [5] have used the K-means clustering algorithm to extract the white blood cells from the blood smears. A typical blood sample contains a lot of other substances like red blood cells, platelets along with white blood cells. So in that case, it is very important to extract only the white blood cells and use it for classification. The proposed method was used to segment the white blood cells in the blood smear and classifying it with CNN achieved an accuracy of 95.81% which upon fine-tuning reached a maximum of 98.96% [4].

2.1.3 *One vs All classification*

Classification of three or more classes can be termed as a ‘multi-class’ classifying problem. One vs All (OVA) is one of the powerful approach to tackle this problem. One particular class trained to distinguish from the rest. As suggested by Rifkin and Klautau in [15], OVA is a powerful technique to increase the accuracy in multi-class classification. The authors have shown that OVA has given better or at least on par results compared to other techniques employed in a multi-class classification problem[15]. Hence, with the thesis also involving multi-class classification, we feel it worth seeing the performance using this approach.

2.1.4 *Multi-channel neural networks*

A novel method proposed by Hu et al. in [19] to classify fMRI brain scan 3D images using multiple channels in 2D CNN has given very promising results. The 2D CNN model will be given multiple 2D images as input with respect to the number of channels that are used. The information is later integrated using a fully connected neural network. The authors have compared these results with SVM, MLP, 2D CNN and, 3D CNN with the M2D CNN. M2D CNN has achieved the highest accuracy amongst the other techniques and also makes over-fitting less severe.

Input data for this thesis contains 37 different images of a cell. It is important to investigate the performance of a model that uses most of these images. Hence using the M2D CNN approach by combining multiple images we are exploring a new approach in WBC classification using CNNs.

2.1.5 *Multi-input neural networks*

This method proposed by Sun et al. in [20] to grade the quality of flowers based on images. The authors are classifying the flowers into three grades i.e three classes. They have implemented single-input CNN as well as a multi-input CNN. On comparing the results of both the approaches, multi-input CNNs have performed better with increased accuracy of 5% that the single input CNNs.

Since our thesis also involves implementation of single input CNN we feel that it is worth investigating the performance of multi-input CNN with our data.

2.2 NOVELTY

Most of the research in the field of artificial intelligence on analyzing white blood cells is done using a small set of stained blood smear

sample images. The machine learning or deep learning models for classification WBC generally use a single image as input. We trying to explore a few techniques where we can use multiple images as input.

The novelty of this project would be to test and evaluate the performance of the techniques discussed in sections [2.1.3](#), [2.1.4](#) and, [2.1.5](#) in WBC classification. We feel that it is a responsibility to make the WBC classification as precise as possible since it can be used for various medical diagnosis. Hence, by trying some less explored techniques in WBC classification we hope to increase the performance and showcase better results.

METHODOLOGY

3.1 PREFACE

From the reference literature we have studied about different methods used to build a model using CNN for image classification. This section focuses on the design and CNN architecture implemented in this thesis.

Most of the WBC classification models use images of stained blood smears or generic white blood cells images found in the internet as shown in figure 3 as the input data.

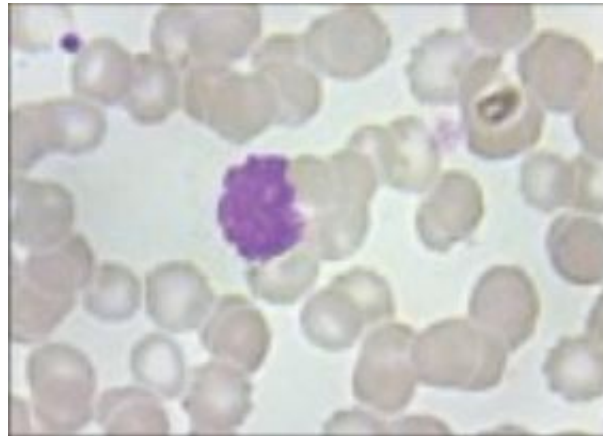


Figure 3: Image of a stained blood smear with a WBC [7].

The data provided by the company is taken from patients and is pre-processed in the HemoCue®WBC DIFF System [2] before we can use it for the model. The blood is drawn into a microcuvette. The chemicals present in the microcuvette rupture the red blood cells and dye the white blood cells so that it will be visible to camera.

The image processing data flow from the instrument is shown in figure 4. The auto focus camera takes the images of the white blood cells in the particular sample at different focal lengths. In the end, the 37 images at the different focal lengths are stacked one upon the other as shown in figure 5.

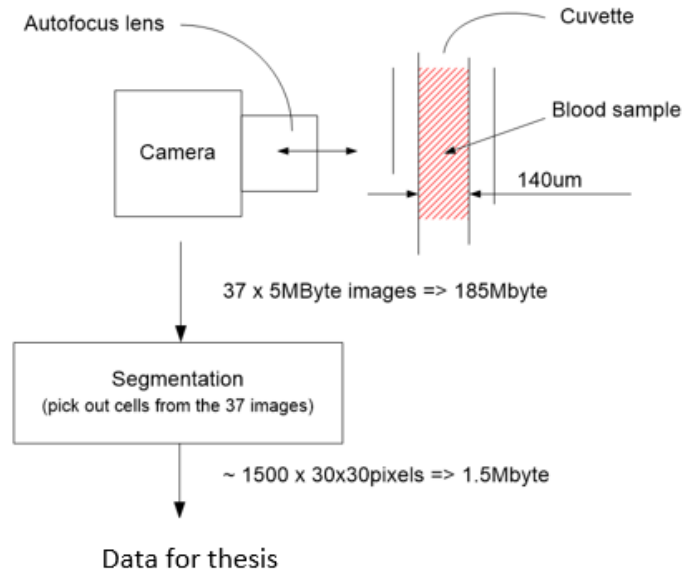


Figure 4: Flow diagram of WBC image processing inside HemoCue® WBC DIFF System.

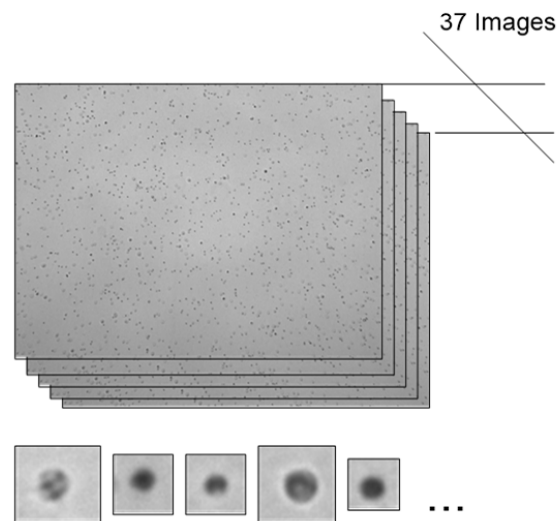


Figure 5: The above image represents a set of stacked images with different focal lengths building up-to the image representation of the given blood sample. The small dots in the images are WBCs, exemplified by the five smaller (zoomed in) images in the bottom row.

For every identified WBC in the sample there is one image plane that corresponds to the best-focused image. For all of the identified WBCs in a given blood sample all 37 image planes are stored with an indication of the best-focused plane, as illustrated in figure 6. For the final representation of a WBC, an additional number of planes are created (see next section).

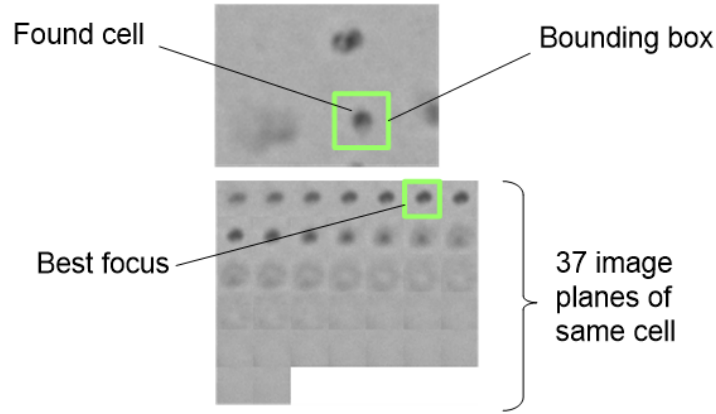


Figure 6: For each found WBC in the blood sample a bounding box is created. The smaller images within the bounding box forms the stack of 37 images for this WBC. Within that stack, the best-focused image plane is identified.

3.2 DATA COLLECTION

The data used in this project was manually labelled by experts, looking at each image and identifying whether it was single, double, triple or trash cell, and identifying cell type. These manually classified images were used for training the different models. 442,130 WBC images were received, and each such image is a stacked TIFF image with 46 different data planes, out of which 37 images corresponds to the previously described focus planes, see figure 5. Nine additional images, developed by the company, were added to the TIFF stack and they contain processed information regarding the identified WBC. Details of top five image planes in the image stack are: Image plane 1 is a combination of the segmented image and the binary raw image. Image plane 2 is the focused grayscale WBC image. Image plane 3 is the binary mask for the focus WBC image. Image plane 4 is the binary mask for the min-image objects used for labeling of the objects. The surrounding objects are removed. Image plane 5 is the binary mask for the min-image objects used for labeling of the objects. The surrounding objects are included. Each image in the TIFF stack has the size 48X48 pixels.

Table 1 shows the details of how 442,130 images are used in for different tasks. In the table the word ‘samples’ refer to the blood samples taken by the company for analysis. Each sample contains images of single cells, double cells, triple cells and trash. The images of single cells further have the labels of monocytes, lymphocytes, neutrophils and eosinophils. The images that are used in systematic error correction is not used training the model. Images in systematic error correction part is first classified into single cells, double cells, triple cells, and trash using our trained algorithm and the total count of WBC is calculated. Total count of WBCs for the same set of images used in systematic error correction is calculated using the Sysmex XN-100 analyser, which is taken as the reference. The images in verification samples are used for final testing our final model. Hence, these images are not used in training of the models.

TYPE	DATA	IMAGES
WBC identification (Single,Double,Triple,Trash) Total data for WBC identification	Train	17551
	Validation	3683
	Test	3692
		25106
WBC differential classification(Single cells) Total data for WBC identification	Train	5459
	validation	1157
	Test	1157
		7773
Systematic error correction Verification	Samples (120)	204654
	Samples	204777
Total thesis data		442130

Table 1: Description of the data received.

The examples of single cells (figure 7), double cells (figure 8), triple cells (figure 9), trash (figure 10) which are used for the estimation of WBC count in the given blood sample. The single cells are further classified into eosinophil (figure 12), lymphocyte (figure 13), monocyte (figure 14), and neutrophil (figure 11).

3.2.1 Training and Validation split

A total of 25,106 images which is used for cell identification is approximately split into 70% training, 15% validation, and 15% testing. 17,551 images are used for training of the initial four classes i.e single cells, double cells, triple cells and, trash. Figure 15 demonstrates the

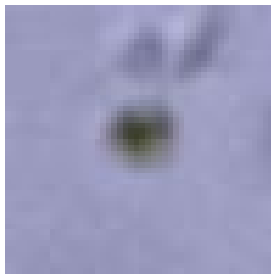


Figure 7: Single blood cell.

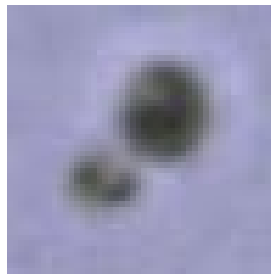


Figure 8: Double blood cell.

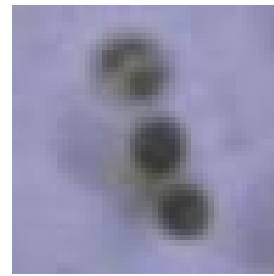


Figure 9: Triple blood cell.



Figure 10: Trash.

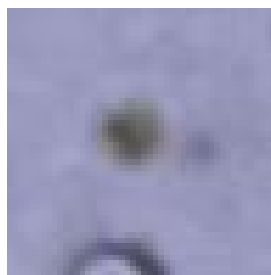


Figure 11: Neutrophil.

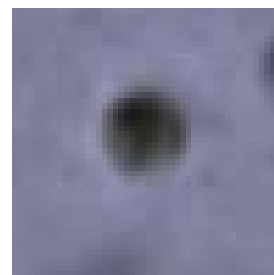


Figure 12: Eosinophil.

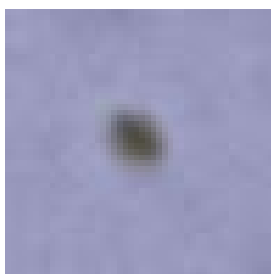


Figure 13: Lymphocyte.

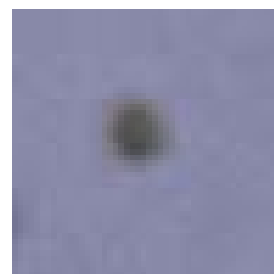


Figure 14: Monocyte.

amount of training data for blood cell identification. Figure 16 demonstrates the amount of training data for the WBC classification.

3.3 PRE-PROCESSING

The labeled data for the few classes triple, double, lymphocyte, and monocyte are less compared to the other classes. In order to avoid under-fitting due to lack of data in few classes the data is augmented for these classes. Basic augmentation techniques like rotations and flips are employed for the classes which contain less training data. Two types of rotations 90 degrees, 180 degrees and, left to right flip are used for data augmentation. Training data of the classes doubles, triples, lymphocytes and monocytes are increased. Further, one hot encoding is used to convert the categories into machine readable format. Figures 17 and 18 show the amount of training data increased after image augmentation.

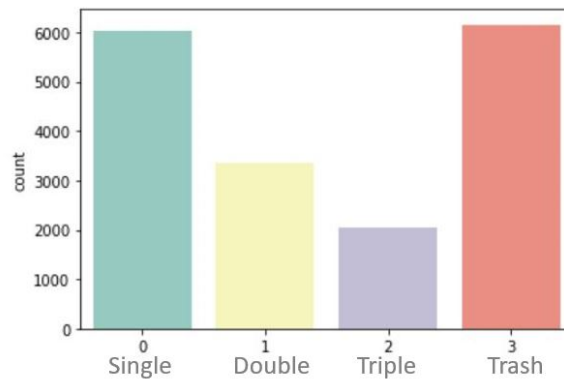


Figure 15: Training data for WBC identification.

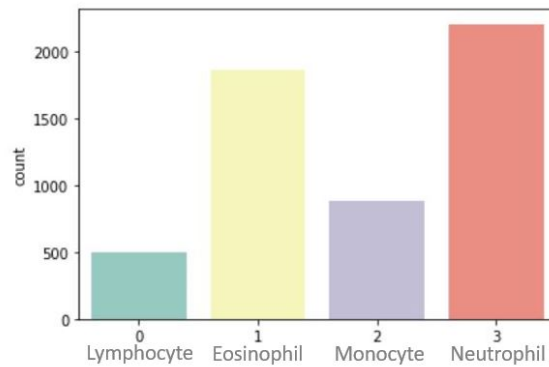


Figure 16: Training data for WBC classification.

3.4 DESIGN

This section describes the design of different models that we propose to achieve the aim of the thesis. As discussed in the earlier sections, this thesis is divided into two significant parts i.e WBC identification and WBC differential classification. The coming sections explain the classification design approaches explored using CNN in the aforementioned parts of the thesis.

3.4.1 WBC identification

This part involves identifying WBCs and estimating the correct amount of WBC in a given sample. There are 4 significant classes - Singles([figure 7](#)), Doubles([figure 8](#)), and so on.

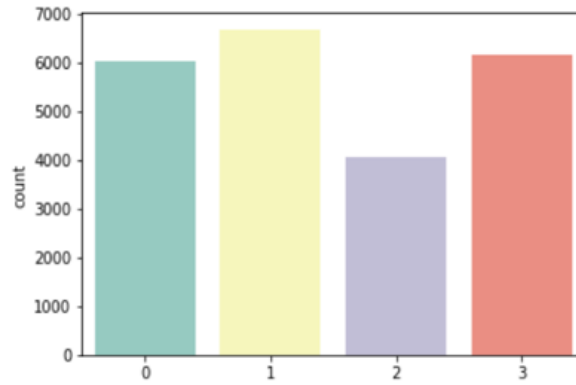


Figure 17: Cell identification data after image augmentation.

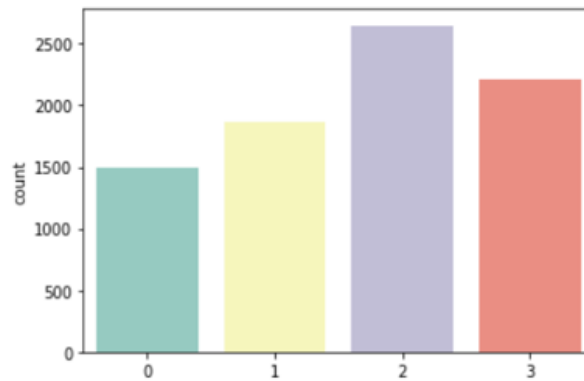


Figure 18: Cell differential data after image augmentation.

4-class CNN cell classification

This is a straightforward approach in which all the four classes are classified together using a single convolutional neural network. Figure 19 depicts the design of this approach.

The training data of the blood samples containing four classes are fed into a single convolutional network after the data pre-processing. As the kernel passes over the images neural network learns the features of four different classes and classifies them.

$$\text{Total WBC count} = \text{single cells} * 1 + \text{double cells} * 2 + \text{triple cells} * 3 + \text{Trash} * 0 \quad (1)$$

This total count of WBC that is calculated might not be accurate due to systematic loss of some WBCs (see section systematic error correction below). Hence a systematic error correction technique is used to correct the total count of white blood cells.

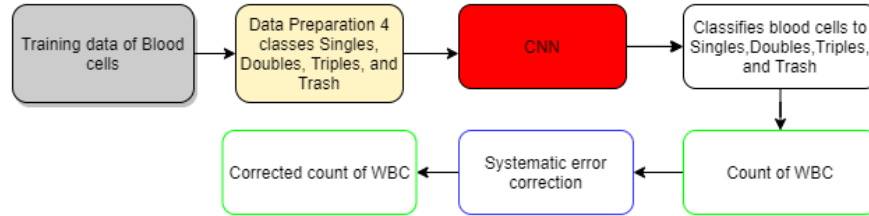


Figure 19: Model flow diagram of 4-class WBC classification.

OVA and 3-class CNN cell classification

When the images of single, doubles, triples and, trash are observed, identification of a single cell amongst others is easier. The identification doubles, triples and, trash require the neural network to learn more features. Also, it is important to achieve high accuracy in classification of single cells since they are further used in differential classification of WBC. Also, authors Rifkin and Klautau in [15] have shown that the OVA approach have given better results in a multi-class classification problem. Hence, we are separating singles and classifying them against the rest of the three classes by grouping the double cells, triple cells and, trash as one class.

This design approach involves two different convolutional neural networks. One convolutional neural network is built for the classification of single white blood cells and others. The other neural network is built for the classification of doubles, triples, and trash. Further on the test samples these two neural networks work together to give the final count of the WBC. Figure 20 depicts the design of this approach.

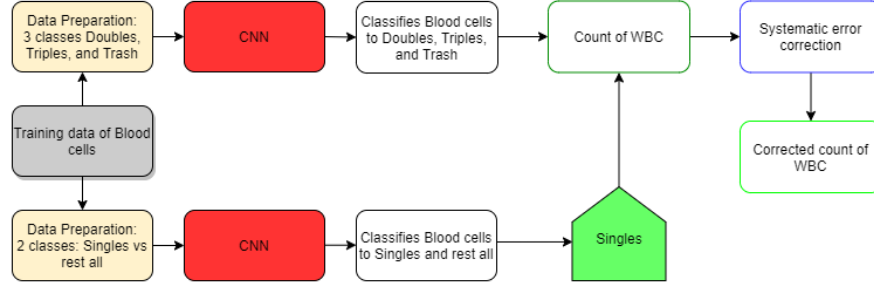


Figure 20: Model flow diagram of OVA and 3-class WBC classification.

Systematic error correction

There is a pessimistic impact on the total count of WBC that is calculated. This impact is due to the loss of data that occurs when the cell falls around the edges in an image from a sample. Images with the incomplete image of a cell is not considered for the total count of WBC which impacts the final count of WBC calculated from our algorithm. Hence, we are proposing a systematic error correction method for the total count of WBC.

A part of the data set (around 120 samples) is taken and the total count of WBC in those samples is calculated using an analyzer "Sysmex XN-1000" from Sysmex Corp. This count is taken as the reference. The total WBC count for the same samples is calculated using our proposed algorithm. The resulting scatter plot (figure 20) can then be used to derive a correction that depends on the estimated WBC count.

The systematic error correction is found by fitting a polynomial, see equation 2, to the scatter plot. A third degree polynomial equation gave us better count which is near to the reference count. A scatter plot of predicted WBC count against the reference WBC count before and after systematic error correction is plotted as shown in figure.

21.

$$\text{Error correction equation} = 0.0005 * \text{WBC}^3 - 0.0044 * \text{WBC}^2 + 0.7887 * \text{WBC} + 0.046 \quad (2)$$

3.4.2 WBC differential classification

In this part, different types of white blood cells are classified. There are five major types of white blood cells. Basophils are a type of WBC whose presence in the human body is only around 0.5% to 1%. This poses a challenge to collect sample data from them. Hence, the four classes that we are classifying are - Neutrophils (figure 11), Lymphocytes (figure 13), Monocytes (figure 14), and Eosinophils (figure 12).

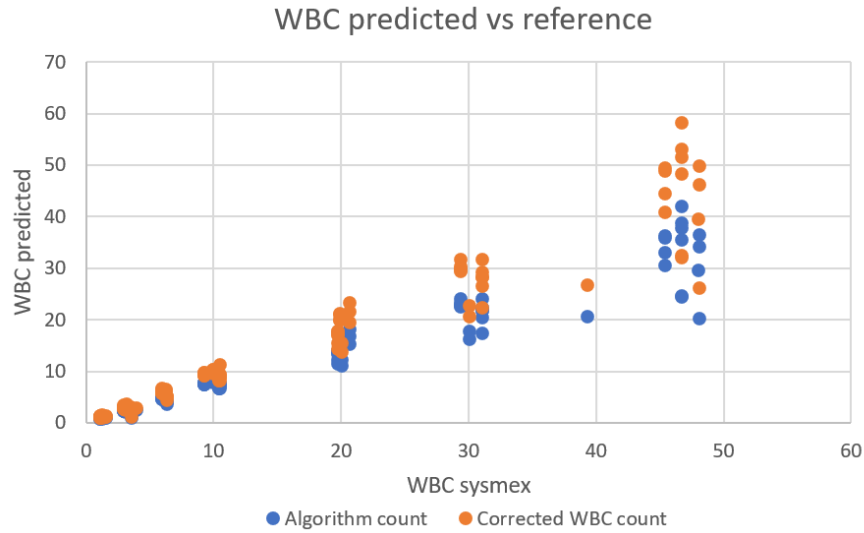


Figure 21: Plot of initial total WBC count vs corrected WBC count.

Similar classification approaches as proposed in the section 3.4.1 are used in the differential classification of WBC.

4-class CNN differential classification

We are using a single convolutional neural network for classifying the types of white blood cells. Figure 22 describes the design of this approach. As discussed in the section 3.3, the training data of the class monocytes is increased.

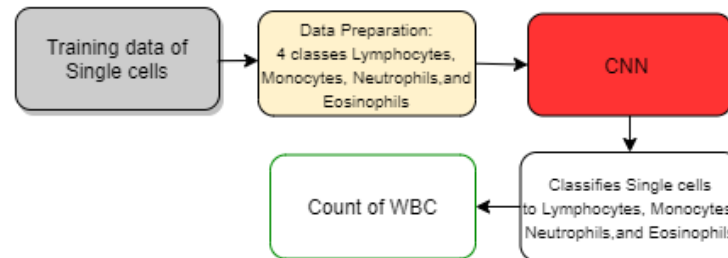


Figure 22: Model flow diagram for 4-class WBC differential classification.

OVA and 3-class CNN differential classification

Upon keen evaluation of the classification results given by our proposed 4-class CNN differential classifier and the classification results of the company, we could observe that the class monocytes had less accuracy percentage than the rest of the classes. These results are shown in the section 4.

This approach is proposed with a purpose to achieve better performance than the 4-class differential classifier especially w.r.t the class

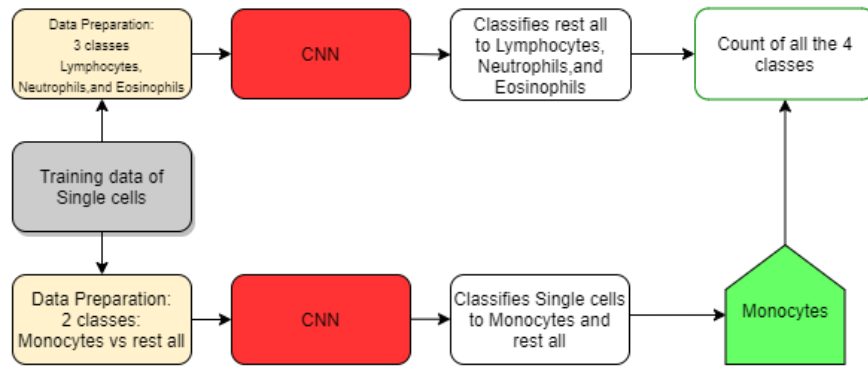


Figure 23: Model flow diagram of OVA and 3-class WBC differential classification.

monocytes. Here two convolutional neural networks are used. One CNN for the classification of monocyte and the rest. The other CNN for classifying neutrophils, lymphocytes and, eosinophils. Figure 23 describes the design of this classification approach.

3.5 ARCHITECTURE

3.5.1 Convolutional neural network

Convolutional neural networks (CNN) are hierarchical neural networks which extract localized features from input images by convolving over the image with a kernel. The use of CNN for image classification on the benchmark MNIST data has have shown fine performance, which is similar to the data used in our thesis (grayscale and binary). Typically, the convolutional neural network architecture comprises of many layers. The input images are passed through the layers of the network like the image pre-processing layer, convolutional layer, pooling layer and, dense layers. Figure 24 depicts the architecture of one of our models used during the training process[12].

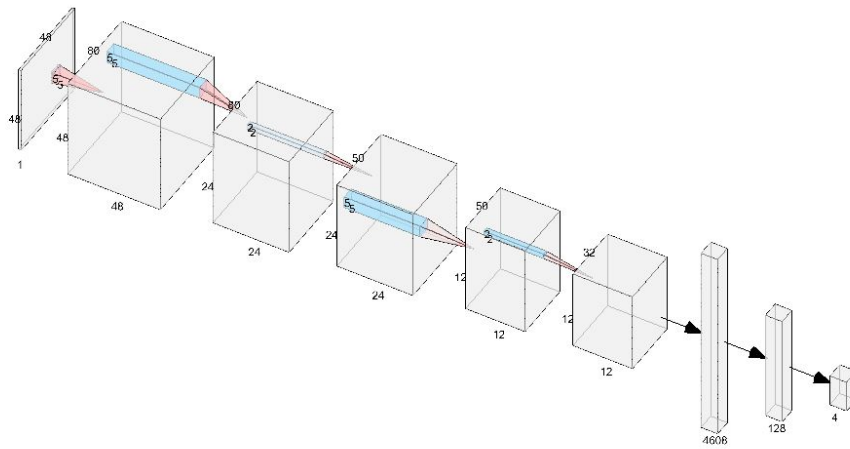


Figure 24: Visualization of an example CNN architecture.

Convolutional layer

The convolutional layers produce a feature map using filters. Filters (small squares) traverse over the input images. The element involved in convolutional operation is the kernel/filter[12].

Kernel and stride selection

The Kernel determines the height and width of the pixels for the feature extraction and strides determine the length of the next step in the image for the kernel to move. the kernel generally moves from left to right in the image. Based on the reference from the paper [10] the kernel size chosen is (3,3) and (5,5).

Pooling layer

The pooling layer down samples the input image by factor K_x and K_y along each direction. This layer is useful to extract dominant information. Max pooling returns the maximum value of the pixels in the portion of the image covered by the kernel.[12]

Dense layer

The layers before the dense layer are used for feature extraction. All the extracted features from the convolutional layers are now taken together in the dense layer or a fully connected layer into a 1D feature vector.[12]

Dropout

This layer is used to prevent over-fitting. The hidden layer nodes are randomly set to zero for each new input, during training, see figure 25. The use of dropout with the fully connected and pooling layers has been shown effective.

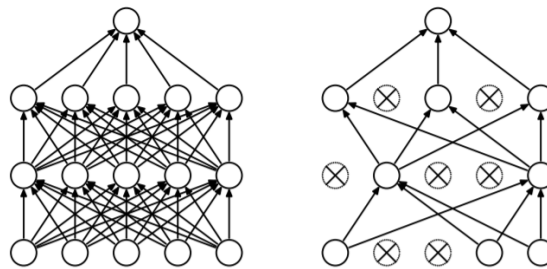


Figure 25: Before and After using dropout.

[14]

Batch Size and Epochs

Batch size is selected to pass the images in batches to the network so that the network could handle it. Epoch is the number of times to run through training data while updating the weights. These are hyper-parameters, see section 4.1.2 for how these are chosen.

3.5.2 Proposed CNN architectural approaches

As the data obtained from the company is in the TIFF format and has a stack of 46 planes of images. Each image plane might contain useful information that can make the classification more accurate. The use of the different layers from the stacked images might result in good feature extraction for the network. Hence we are proposing a couple of methods where we can utilize the different images from the stack of one sample in a convolutional neural network.

The best-focused image of the cell is somewhere in the middle of the stack. Though the images before and after the best-focused image are out of focus, those images also contain information regarding the same cell, and using those images might as well help the neural network to learn more features and thus might result in an effective classification of the cell. The idea is to use these images along with best-focused images in multiple channels in the neural network and as multiple inputs to a neural network.

3.5.3 Multi-channel convolutional neural network classification

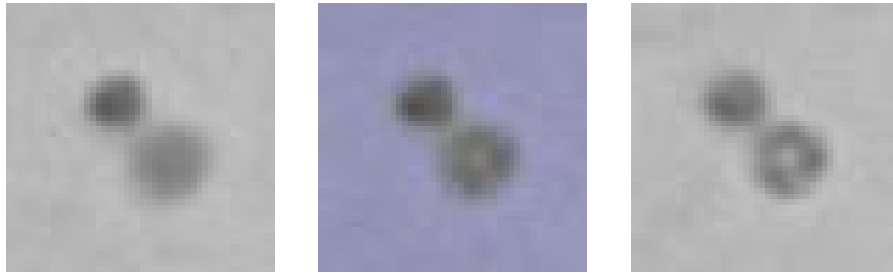


Figure 26: Image before the focused plane.

Figure 27: Plane 1 image in the image stack.

Figure 28: Image after the focused plane.

This method is implemented with a purpose to make the neural network learn more features with the use of multiple images in multiple channels. So, we are using grayscale images before (figure 26) and after (figure 28) the focused image in the image stack (figure 5) of a sample. Along with these images the first image plane, see figure 27. The image stack which is the focused RGB image of WBC with a blue background and the binary mask of the focused image is used.

The proposed use of images requires five channels are to extract the features. The grayscale image before the focused image plane is used in the first channel. Since the first image of the image stack is an RGB image, it requires three channels one for each color component in the image. The image plane after the focused image is used in the last channel of the neural network. This method of using multiple images in multiple channels is illustrated in figure 29.

3.5.4 Multi-input convolutional neural network classification

The implementation of this method also serves the same purpose as the method illustrated in the above section 3.5.3. The only difference is that the image planes shown in figures 26, 27, and 28 are used in three different input layers instead of using them in multiple channels in a single input layer as shown in figure 30. This method could

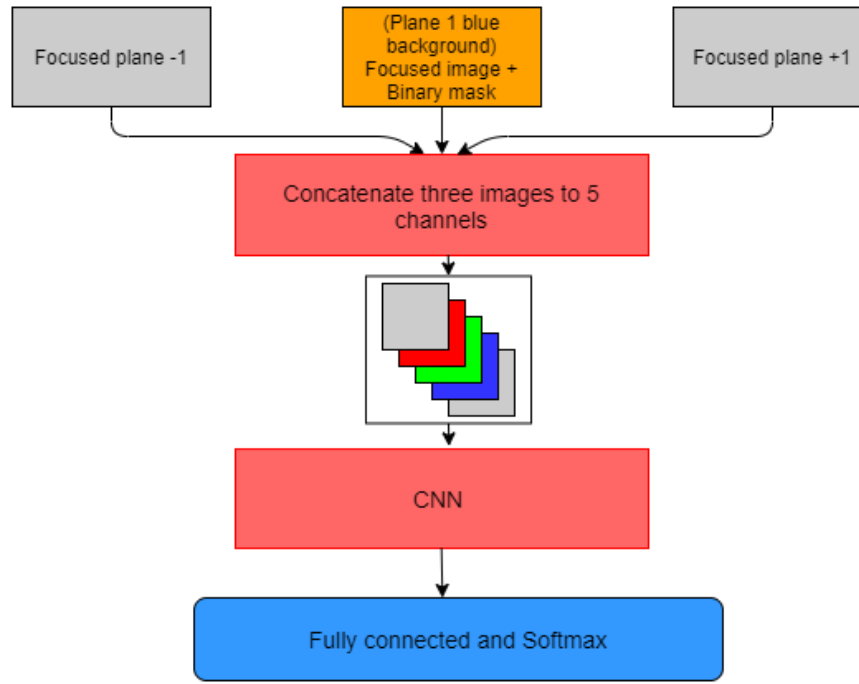


Figure 29: Multi-channel convolutional neural network for cell identification.

be more efficient than the previous mentioned method 3.5.3, as the features are extracted from each input plane then followed by fully connected layers. where as in 3.5.3 the images are concatenated and the feature extraction is done on the whole input in different filters.

The first and last input layers require only one channel as the images used as input are grayscale. The second input layer requires three channels as the first plane image from the image stack used as input is an RGB image. Later the features extracted in these input layers from the different input images of the same sample are concatenated and then are fed to the fully connected network.

3.6 FINAL INTEGRATED DESIGN

In this section, we are proposing our final model for analyzing the white blood cells. This final model is selected based on careful performance evaluation of our proposed classification approaches and the CNN architectural approaches. The final model flow diagram is as shown in figure 31.

Based on our analysis, the classification approach of OVA and 3-class classifier was found to more effective. The proposed CNN architectural approaches were tested. The proposed architectural approaches were giving on par results. The results are shown in the next chapter 4.

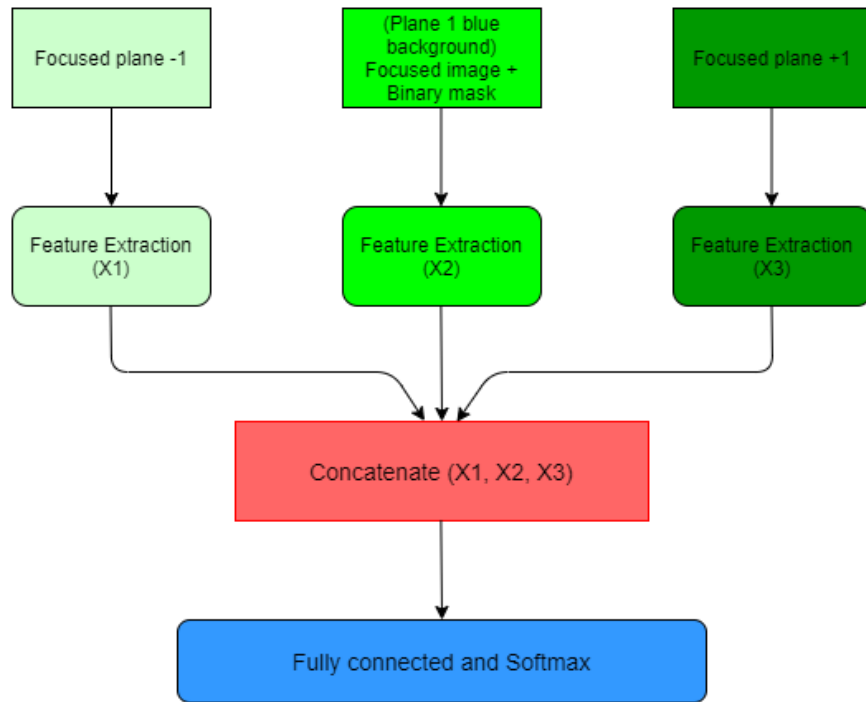


Figure 30: Multi-input convolutional neural network for cell identification.

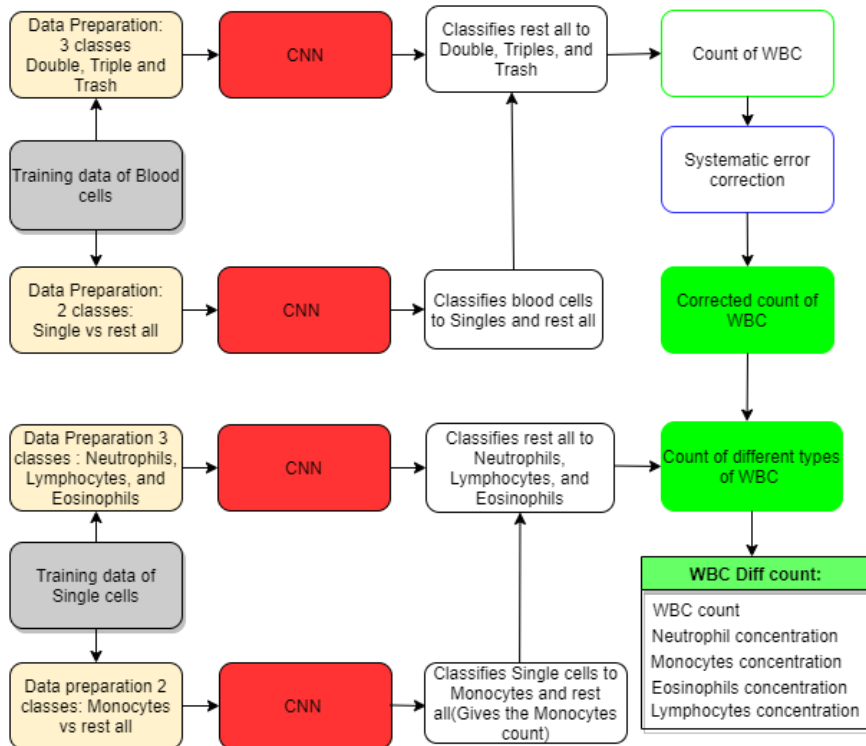


Figure 31: Integrated model flow diagram.

The final integrated model that we want to elucidate follows the approach of OVA classification and single input CNN architecture. The integrated final model incorporated with 4 convolutional neural networks. All the discussed pre-processing techniques utilized and the intended outcomes of this integrated model are - total count of WBCs after systematic error correction and concentration of each type of WBC.

3.7 ASSESSMENT METHOD

The performance of the different classification and CNN architectural approaches are assessed by plotting a confusion matrix. This gives us the number of samples in each class that is wrongly classified. This matrix is also one of the means to compare the performances of our classification model versus the existing model in the HemoCue®WBC DIFF System.

Figure 33 shows a confusion matrix. The dark blue diagonal boxes and the numbers in them represent the percentage of correct predictions whereas the light blue boxes and the white boxes represent the percentage of incorrect predictions.

To explain the terminologies of a confusion matrix, let us take the example of cell identification which consists of four classes - singles, doubles, triples and, trash. When an image from 'singles' is classified correctly under 'singles' then it is termed as true positive(TP) but if it is classified under 'doubles' it is termed as false negative(FN). When an image that does not belong to the class 'singles' and is not classified under the class 'singles', then it is termed as true negative(TN) but if classified under the class 'singles' then it is termed as false negative(FN)[21].

Using the above-mentioned terminologies it is possible to evaluate the performance of the model. 'Recall' or 'True positive rate' or 'Sensitivity' is the ability of the model to find all the true positives. It is calculated using the equation 3. If recall indicates the rate of true positives in a model, 'Precision' represents the proportion of true positives that were actually true positives. It is calculated using equation 4. F1-score is a measure of model accuracy on a data set and it is calculated by taking the harmonic mean of precision and recall 5.

$$\text{Recall} = \text{TP} / (\text{TP} + \text{FN}) \quad (3)$$

$$\text{Precision} = \text{TP} / (\text{FP} + \text{TP}) \quad (4)$$

$$\text{F1 - score} = 2 * (\text{Precision} * \text{Recall}) / (\text{Precision} + \text{Recall}) \quad (5)$$

The performance of classifiers cannot be determined based on the individual class values of recall, precision, and F1-score. False positives and false negatives are also crucial in a classification problem like in the case of classification of WBC. Accuracy is a performance metric used when true positives and true negatives are of more importance, whereas F1-score is a performance metric which gives more importance to false positives and false negatives.

The classes being imbalanced, it is also important to address this imbalance when we calculate our performance metric. Hence, we propose to calculate weighted-average based recall, precision, F1-score. Weighted average is the sum of all class samples multiplied by its weight divided by the total number of samples[29].

3.8 HARDWARE

The algorithms were trained on a computational server and laptop with the following hardware specifications.

3.8.1 *Laptop*

- GPU: NVIDIA GTX 1080 Ti (8GB) - CUDA cores:3584
- CPU: Intel i7-7700HQ @ 3.81GHz (Overclocked)
- RAM: 16GB 1600MHz

3.8.2 *Computational server*

- GPU: NVIDIA RTX 2080 Ti (11GB) - CUDA cores:4352
- CPU: Intel i9-9900X @ 3.50GHz (Base clock)

RESULTS AND ANALYSIS

4.1 ANALYSIS

4.1.1 Loss and Accuracy curves

One way of evaluating the models built with the proposed methodology is by plotting the model loss and model accuracy of the training set and the validation set. These learning curves can be used to detect an over-fit, under-fit ,or a well-fit model.

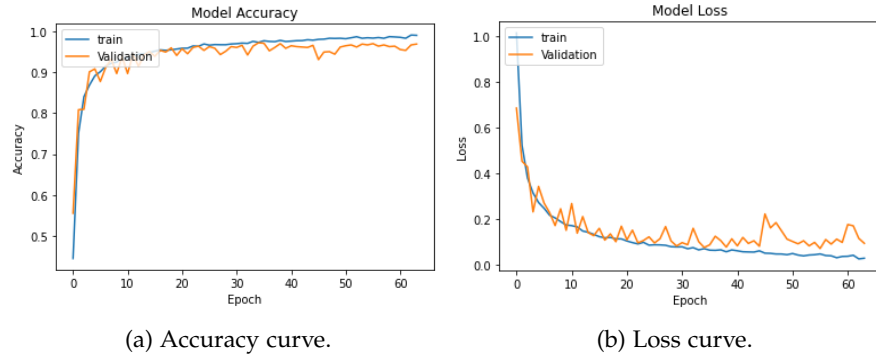


Figure 32: Accuracy and Loss curves of 3-class differential model.

The loss and accuracy curves in figure 31 in demonstrates a good fit. The validation loss curve decreases to the point of stability and has a small gap with the training loss. The training curve for the validation shows similar properties where it increases to the point of stability and has a small gap with the training accuracy. The above plots 32b and 32a are for one of the best models that we are using in the final design.

4.1.2 Hyper-parameter selection

Hyper-parameters control the behaviour of the model. A variety of hyper-parameters could be chosen to optimize a CNN based on the application and the data. These hyper-parameters affect different aspects of the network like the architecture, the optimization process and the handling of the data. The following table lists the some of the important hyper-parameters that are tuned for the model that is used in the final integrated design 3.6.

The best hyper-parameters are chosen manually for each of the models mentioned in the section 3 from the minimum to maximum range

Method	#	Hyperparameter	min	max	best in WBC identification	best in WBC DIFF identification
OVA	1	No. of convolutional layers	1	5	4	2
	2	Kernel size	1	7	3 and 5	3
	3	Stride	1	3	1	1
	4	Pooling	-	-	Max pooling	Max pooling
	5	Dropout percentage	0.1	0.9	0.5	0.5
	6	Activation function	-	-	ReLU	ReLU
	7	Number of dense layers	1	5	2	3
	8	Size of each dense layer	1	2048	128,2	256,512,2
	9	Epochs	10	60	29	35
3 Class CNN	1	No. of convolutional layers	1	5	3	3
	2	Kernel size	1	7	3	3
	3	Stride	1	3	1	1
	4	Pooling	-	-	Max pooling	Max pooling
	5	Dropout percentage	0.1	0.9	0.5	0.5 and 0.4
	6	Activation function	-	-	ReLU	ReLU
	7	Number of dense layers	1	5	3	3
	8	Size of dense layers	1	2048	128,128,3	1024,512,3
	9	Epochs	10	60	45	45

Table 2: List of set hyper-parameters for the OVA and 3-class classification model.

mentioned in table 2. Hyper-parameters like kernel size, stride, and pooling are set for each convolutional layers.

Hyper-parameters are also selected based on different training and validation runs. During each of the training and validation runs the combination hyper-parameters listed in table 2. The set of hyper-parameters yielding the best performance is noted and is used in the final integrated model.

4.2 RESULTS

4.2.1 Accuracy

Accuracy is one of the metric used to evaluate the performance of the different approaches.

Tables 3 and 4 shows the number of parameters along training, validation, and test accuracy percentages from different methods that were tested in the WBC identification part and the WBC differential classification part. We can observe that the number of parameters increases in multi-channel and multi-input approaches. The lesser difference between the training and validation accuracy indicates a reduced risk of over-fitting. Also, the OVA and 3-class classification approach with a test accuracy of 95.45% in cell identification part and 90.49% in cell differentiation turns out to be the most accurate approach.

Methods for WBC identification	Number of parameters	Train Accuracy	Validation Accuracy	Test Accuracy
4 Class CNN - Plane1	520,132	0.95	0.91	0.92
4 Class CNN - Multi-channel	20,430,595	0.94	0.90	0.92
4 Class CNN - Multi-input	15,390,308	0.96	0.91	0.93
OVA and 3 Class CNN - Plane1	1,410,980	0.97	0.94	0.95
OVA and 3 Class CNN - Multi-channel	44,520,708	0.95	0.91	0.92
OVA and 3 Class CNN - Multi-input	37,897,708	0.96	0.90	0.93

Table 3: Classification results for different methods in WBC identification part.

Methods for WBC Differential count	Number of parameters	Train Accuracy	Validation Accuracy	Test Accuracy
4 Class CNN - Plane1	520,132	0.95	0.91	0.84
OVA and 3 Class CNN - Plane1	1,410,980	0.97	0.94	0.94

Table 4: Classification results for different methods in WBC Differential part.

4.2.2 Confusion Matrix

As explained in 3.7, the confusion matrix is another way of assessing the performance of our classification methods, as shown in figure 33. This confusion matrix can be evaluated using the 'False Positives', 'False Negatives', and 'True Positives' from each of the confusion matrices.



Figure 33: Example of a confusion matrix from our final model OVA 4-class CNN classifier.

Method	Class	TP	FP	FN	TN
4 Class CNN - Plane1	Single	1221	40	26	2361
	Double	571	10	94	2951
	Triple	418	73	68	3195
	Trash	1213	42	37	2394
4 Class CNN - Multi channel	Single	1234	62	51	2339
	Double	566	114	99	2907
	Triple	404	78	82	3204
	Trash	1200	28	50	2408
4 Class CNN - Multi input	Single	1221	30	64	2371
	Double	593	109	72	2984
	Triple	428	60	58	3198
	Trash	1213	32	37	2441
OVA and 3 class CNN - Multi channel	Single	1221	52	64	2349
	Double	565	108	100	3013
	Triple	437	84	49	3165
	Trash	1200	19	50	2717
OVA and 3 class CNN - Multi input	Single	1234	52	51	2349
	Double	572	114	93	3000
	Triple	423	65	63	3135
	Trash	1201	25	49	2411
OVA and 3 Class CNN - Plane1	Single	1246	20	39	2381
	Double	592	72	53	2949
	Triple	447	73	39	3166
	Trash	1225	11	25	2425

Table 5: Results from confusion matrices of different design methods in WBC identification.

Method	Class	TP	FP	FN	TN
4 Class CNN - Plane1	Eosinophil	99	0	6	1180
	Lymphocyte	443	55	33	754
	Monocyte	98	38	95	1149
	Neutrophil	445	107	66	667
OVA and 3 Class CNN Plane1	Eosinophil	101	0	4	1180
	Lymphocyte	471	13	5	610
	Monocyte	158	16	35	1111
	Neutrophil	485	41	26	759

Table 6: Results from confusion matrices of different design methods in WBC differential classification.

Table 5 gives the results of the different models used to achieve WBC count and table 6 gives the results of the models used to identify the WBC differential cells count.

Performance metrics

Figures 17 and 18 indicate the classes are slightly imbalanced and it is important to evaluate the classifiers taking in to account this imbalance. Hence we propose to evaluate the classifiers based on weighted average [29]. Using absolute values from tables 5 and 6 we are calculating 'weighted-average precision', 'weighted-average recall' and 'weighted-average f1 score'.

By calculating the weighted average threshold metrics using the absolute values of TP/TN/FP/FN to sanity-check the numbers. Weighted average numbers could tackle the imbalance in the classes by we have calculated the weighted-average precision, recall and the F1 score to be able to show the classifier having the higher weighted-average F1 score has performed well.

Method	Class	Recall	Specificity	Precision	F1-score
4 Class CNN Plane1	Single	0.97	0.98	0.96	0.97
	Double	0.85	0.96	0.84	0.84
	Triple	0.86	0.97	0.85	0.85
	Trash	0.97	0.98	0.96	0.96
4 Class CNN Multi channel	Single	0.96	0.97	0.95	0.95
	Double	0.85	0.96	0.83	0.84
	Triple	0.83	0.97	0.83	0.83
	Trash	0.96	0.98	0.97	0.96
4 Class CNN Multi input	Single	0.95	0.98	0.97	0.96
	Double	0.89	0.96	0.84	0.86
	Triple	0.88	0.98	0.87	0.87
	Trash	0.97	0.98	0.97	0.97
OVA and 3 class CNN Multi channel	Single	0.95	0.97	0.95	0.95
	Double	0.84	0.96	0.83	0.84
	Triple	0.89	0.97	0.83	0.86
	Trash	0.96	0.99	0.98	0.97
OVA and 3 class CNN Multi input	Single	0.96	0.97	0.95	0.95
	Double	0.86	0.96	0.83	0.84
	Triple	0.87	0.97	0.86	0.86
	Trash	0.96	0.98	0.97	0.97
OVA and 3 Class CNN Plane1	Single	0.96	0.99	0.98	0.97
	Double	0.91	0.97	0.89	0.90
	Triple	0.91	0.97	0.85	0.88
	Trash	0.98	0.99	0.99	0.98

Table 7: Performance metrics for different methods in cell identification

Method	Class	Recall	Specificity	Precision	F1-score
4 Class CNN Plane1	Eosinophil	0.94	1	1	0.97
	Lymphocyte	0.93	0.93	0.88	0.90
	Monocyte	0.50	0.96	0.72	0.59
	Neutrophil	0.87	0.86	0.80	0.83
OVA & 3 Class CNN Plane1	Eosinophil	0.96	1	1	0.98
	Lymphocyte	0.98	0.97	0.97	0.98
	Monocyte	0.81	0.98	0.90	0.86
	Neutrophil	0.94	0.94	0.92	0.93

Table 8: Performance metrics for different methods in cell differentiation

Method	Weighted-avg Recall	Weighted-avg Precision	Weighted-avg F1-score
4 Class CNN - Plane1	0.93	0.92	0.93
4 Class CNN - Multi channel	0.92	0.92	0.92
4 Class CNN - Multi input	0.93	0.93	0.93
OVA and 3 Class CNN Multi channel	0.92	0.93	0.92
OVA and 3 Class CNN Multi input	0.93	0.93	0.93
OVA and 3 Class CNN Plane1	0.95	0.95	0.95
4 Class CNN - Differential Plane1	0.85	0.87	0.86
OVA and 3 Class CNN - Differential Plane1	0.94	0.95	0.94

Table 9: Weighted-average performance metrics for different methods

Tables 7, 8 and 9 show different threshold metrics calculated for different models. We also evaluate the models based on the highest weighted-average F1-score. Table 9 indicates that the 'OVA and 3-class CNN using plane-1 image' which is used in our final integrated design has the highest weighted average F1-score of 0.9551 for cell identification and 0.9496 for cell differentiation.

4.2.3 Verification plot

The verification plot is plotted to verify the performance of the final integrated design. A graph of error percentage against the total count calculated from the 'Sysmex XN-100' analyzer is plotted to verify the performance of our design. The figure 34 describes the performance

of the OVA and 3 Class approach by plotting the samples count with reference to the count of the WBC from 'Sysmex XN-100'. The error is calculated by taking the difference between predicted and the reference. The reference count of the WBC is provided by the company for the comparison. The plot is divided into 2 regions with error per-

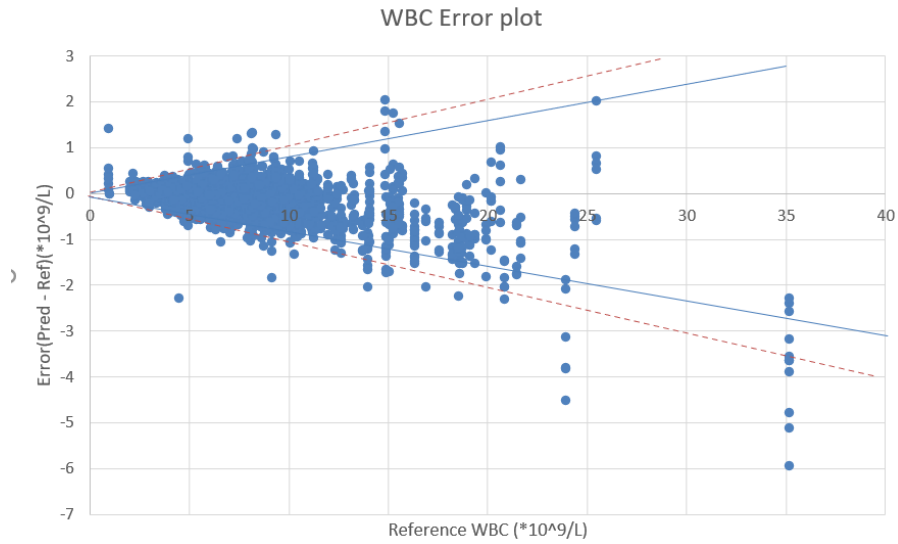


Figure 34: Verification plot of OVA and 3-class classifier.

centages varying from 10% - red dotted line and blue dotted line is plotted by calculating the error percentage line covering 95% of the samples. The blue line corresponds to 9.2% error. The final integrated design of OVA and 3-class classifier is used for this verification plot. The performance of the algorithm is measured by how low is the error percentage for 95% samples. It is important as per industry standards that at least 95% of the samples classified from our neural network are inside the 10% error range. In the verification plot shown in 34, 96.7% are inside the 10% error range.

DISCUSSION

With the proposed final integrated design for identification of WBC, calculating the total count of WBC and classification of different types of WBCs we have shown satisfying results. Now in this section, we will scrutinize our results from section 4.

5.1 INTERPRETATION

Interpretation of each of the design approaches alongside the aim of the thesis, the approach of 'One vs All and 3-class classification' fared better than the rest of the approaches we have explored. On analyzing our results we can also interpret that the use of image planes before and after the focused image plane of WBC did not help in enhancing the performance of the neural network.

It is important to note the use of the image from the first plane from the image stack, see in figure 5, in all our proposed approaches. Plane-1 image is built by combining the focus image of the cell with the binary mask of the focus image and might be one of the influencing factors for effective classification. The use of just the focused image or the segmented image of the focused image has not yielded good results compared to the performance using the plane-1 image. Binary mask defines the region of interest of the original image[28]. The region of interest in our case is the focused white blood cell region. Hence by defining this region of interest along with the focused image in the plane-1 image is improving the cell identification compared to the use of focused image that is found in the middle of image stack.

5.1.1 OVA and 3-class classifier

With convincing related work on OVA classification from [15], we separated one class from each part of the thesis and have classified the remaining three classes in a 3-class classifier. This design technique has resulted in an accuracy of 95.45% on the test data set in the WBC identification part and an accuracy of 90.49% in the differential classification part. This accuracy metric of 'OVA vs 3-class classification' is approximately 4% higher than the traditional multi-class classification and also better than the proposed two architectural approaches for this thesis.

On analysing the confusion matrix for the WBC identification part, the true positive rate for singles is 89% and the precision is 97% which indicates that 97% of true positive samples are actually true positive.

These metrics for the remaining classes are also promising and have better recall and precision numbers than the rest of the design methods in tables 5 and 6.

5.1.2 *Multi-channel and Multi-input architectural design approaches*

One of the reasons why the authors in [19] and [20] achieved better results by employing multi-class and multi-channel methods on their respective classification problems, might be because the authors have used completely different images of a class in multiple channels and as multiple inputs. With the use of different images of a class helps the neural network to learn a variety of features in a class. Whereas, we have used images that are nearly similar. The only difference in the images that we have used is the focal length of the image.

The hypothesis of using images from different planes in the image stack, see figure 6 was to improve the identification of doubles and triples. For example, considering the image stack of double cells there are some instances where in images of each cell in the double cells are found in the adjacent to the best focused image plane in the image stack. Hence with the notion of improving the accuracy in classification of doubles and triples, With the use of slightly out of focus images in the multi-class and multi-channel algorithm has hindered the performance of these algorithms. It is clear that the features learned by the neural network using these images are not useful for classification.

Table 3 shows the number of parameters in each of our proposed methods. The multi-input and multi-channel approaches have far higher parameters than our proposed final integrated design. Taking into account these interpretations multi-input and the multi-channel, we did not proceed to implement these on the differential classification. Yet, we can say that these are powerful CNN methods that are totally worth exploring.

5.1.3 *Basophil concentration*

The training data for the fifth type of blood cell were not provided by the company but it is possible to estimate the concentration of the fifth type of blood cell(basophils) by calculating the difference between the total WBC count and sum of differential cell concentration obtained by the model. Normally, basophils make up less than 1 percent of circulating white blood cells. A healthy range is 0 to 3 basophils in each micro liter of blood. This metric is very low, and it does not impact the testing on a great extent.

5.2 LIMITATIONS

One of the limitations of our thesis is not classifying one of the types of WBC i.e basophils. Due to their scarcity in the human body, it has posed a challenge to classify them. Also, another limitation of this thesis would be the differential classification of the WBC types only in the 'single cells'.

CONCLUSION AND FUTURE WORKS

6.1 CONCLUSION

The work is seen to set a deep learning algorithm for the HemoCue®-WBC DIFF System in giving the total count of WBCs by identifying different kinds of WBCs and then classifying them into four different types. To develop this we have explored two classification approaches and two CNN architectural approaches and evaluated the results.

It might not be wrong to say that the classification approach of 'One vs All' has been a boon to us. An inference we can draw is that the OVA method does improve the accuracy of a multi-class classification problem.

The final integrated design for the HemoCue®WBC DIFF System is built using four neural networks. The OVA method and the 3-class classifier approach have an accuracy of 94% in the WBC identification part which is nearly 3% higher than the rest of the illustrated methods. Whereas, in the WBC differential classification the OVA and 3-class classifier achieves an accuracy of 90.49% which is around 6% higher than the 4-class CNN classifier illustrated for this part.

6.2 FUTURE WORKS

The scope of using deep learning techniques in hematology has a very wide range. Deep learning techniques can also be used to analyze other components of the blood or analyze all components in the blood to get the metrics of each component in the blood sample.

Narrowing down future research scope to deep learning and WBC analysis, we can try the same analysis using region-based convolutional neural network(R-CNN) where the image is divided into regions and then CNN is applied for each region respectively. This might help the network to learn more features and might improve the classification performance. Also, variants if R-CNN like FAST R-CNN can be used where CNN is applied first and then divided into regions. This method is slightly faster than R-CNN. Other deep learning techniques like transfer learning where using a pre-trained model to classifying WBCs can also be explored.

Further, narrowing down the future works specifically in this project, we would like stress in classification basophils. Though they are less in number, upon getting little data we can employ rigorous data augmentation techniques and can improve the number of basophils data for training and then use it for classification. Also, we have a strong

belief that the proposed CNN architectural design methods could give convincing results if it is trained using different images of a WBC blood smear rather than training with grayscale images of WBC varying in focal length.

With the advancement in the field of hematology, it is possible to get access to numerous images related to blood and its components. Convolutional neural networks and different design techniques in CNNs are powerful tools at our disposal. By making good use of these images and we can make wonders in the field of hematology or the healthcare sector on the whole. The show must go on..

BIBLIOGRAPHY

- [1] <https://www.hemocue.com/en/about-us/innovate>
- [2] <https://www.hemocue.com/en/solutions/hematology/hemocue-wbc-diff-system>
- [3] George-Gay, B., Parker, K. (2003). Understanding the complete blood count with differential. *Journal of Perianesthesia Nursing*, 18(2), 96-117.
- [4] Pedersen, K. M., Åolak, Y., Ellervik, C., Hasselbalch, H. C., Bojesen, S. E., Nordestgaard, B. G. (2019). Smoking and Increased White and Red Blood Cells: A Mendelian Randomization Approach in the Copenhagen General Population Study. *Arteriosclerosis, thrombosis, and vascular biology*, 39(5), 965-977.
- [5] Su, M. C., Cheng, C. Y., Wang, P. C. (2014). A neural-network-based approach to white blood cell classification. *The scientific world journal*, 2014.
- [6] Elen, A., Turan, M. K. Classifying White Blood Cells Using Machine Learning Algorithms. *ve Gelistirme Dergisi*, 11(1), 141-152.
- [7] Mathur, Atin et al. Scalable system for classification of white blood cells from Leishman stained blood stain images. *Journal of pathology informatics* vol. 4, Suppl S15. 30 Mar. 2013, doi:10.4103/2153-3539.109883.
- [8] Zheng, Xin Wang, Yong Wang, Guoyou Liu, Jianguo. (2018). Fast and Robust Segmentation of White Blood Cell Images by Self-supervised Learning. *Micron*. 107. 10.1016/j.micron.2018.01.010.
- [9] Lin, L., Wang, W., Chen, B. (2019). Leukocyte recognition with convolutional neural network. *Journal of Algorithms Computational Technology*. <https://doi.org/10.1177/1748301818813322>.
- [10] Li, H., Kadav, A., Durdanovic, I., Samet, H., Graf, H. P. (2016). Pruning filters for efficient convnets. *arXiv preprint arXiv:1608.08710*.
- [11] Loshchilov, I., Hutter, F. (2015). Online batch selection for faster training of neural networks. *arXiv preprint arXiv:1511.06343*.
- [12] Ciresan, D. C., Meier, U., Masci, J., Gambardella, L. M., Schmidhuber, J. (2011, June). Flexible, high performance convolutional neural networks for image classification. In *Twenty-Second International Joint Conference on Artificial Intelligence*.

- [13] Wu, H., Gu, X. (2015). Towards dropout training for convolutional neural networks. *Neural Networks*, 71, 1-10.
- [14] Srivastava, N., Hinton, G., Krizhevsky, A., Sutskever, I., Salakhutdinov, R. (2014). Dropout: a simple way to prevent neural networks from overfitting. *The journal of machine learning research*, 15(1), 1929-1958.
- [15] Rifkin, R., Klautau, A. (2004). In defense of one-vs-all classification. *Journal of machine learning research*, 5(Jan), 101-141.
- [16] F. Jiang et al., "Deep Learning based Multi-channel intelligent attack detection for Data Security," in *IEEE Transactions on Sustainable Computing*.
- [17] Ouyang, Wanli, and Xiaogang Wang. "Joint deep learning for pedestrian detection." *Proceedings of the IEEE International Conference on Computer Vision*. 2013.
- [18] Tan, L., Wang, Q., Zhang, D. et al. Lymphopenia predicts disease severity of COVID-19: a descriptive and predictive study. *Sig Transduct Target Ther* 5, 33 (2020). <https://doi.org/10.1038/s41392-020-0148-4>
- [19] Qin, C., Zhou, L., Hu, Z., Zhang, S., Yang, S., Tao, Y., Xie, C., Ma, K., Shang, K., Wang, W., Tian, D. S. (2020). Dysregulation of immune response in patients with COVID-19 in Wuhan, China. *Clinical Infectious Diseases : an Official Publication of the Infectious Diseases Society of America*. <https://doi.org/10.1093/cid/ciaa248>
- [20] Hu, J., Kuang, Y., Liao, B., Cao, L., Dong, S., Li, P. (2019). A Multichannel 2D Convolutional Neural Network Model for Task-Evoked fMRI Data Classification. *Computational Intelligence and Neuroscience*, 2019.
- [21] Sun, Y., Zhu, L., Wang, G., Zhao, F. (2017). Multi-input convolutional neural network for flower grading. *Journal of Electrical and Computer Engineering*, 2017.
- [22] Tharwat, A. (2018). Classification assessment methods. *Applied Computing and Informatics*.
- [23] George-Gay, B., Parker, K. (2003). Understanding the complete blood count with differential. *Journal of Perianesthesia Nursing*, 18(2), 96-117.
- [24] Huang et al., Clinical features of patients with 2019 novel coronavirus in Wuhan, China. *The Lancet* 2020;395: 497-506.

- [25] W. Guan et al., Clinical Characteristics of Coronavirus Disease 2019 in China. The New England Journal of Medicine 2020, Feb 28.
- [26] Qin C. et al., Dysregulation of immune response in patients with COVID-19 in Wuhan, China. Clinical Infectious Disease 2020, Mar 12
- [27] Huang et al., 2019 novel coronavirus patient's clinical characteristics, discharge rate and fatality rate of meta-analysis.
- [28] [https://se.mathworks.com/help/images/create-binary-mask-from-grayscale-image.html: :text=The%2obinary%2omask%20defines%20a,is%20part%20of%20the%20background.](https://se.mathworks.com/help/images/create-binary-mask-from-grayscale-image.html#:text=The%2obinary%2omask%20defines%20a,is%20part%20of%20the%20background.)
- [29] Behera, B., Kumaravelan, G. (2019, December). Performance Evaluation of Deep Learning Algorithms in Biomedical Document Classification. In 2019 11th International Conference on Advanced Computing (ICoAC) (pp. 220-224). IEEE.



DECLARATION

DECLARATION

This thesis is a presentation of our original research work. Wherever contributions of others are involved, every effort is made to indicate this clearly, with due reference to the literature.

_____ Suraj Neelakantan and Sai Sushanth Varma Kalidindi



Suraj is a machine learning enthusiast, inquisitive about medical applications of machine learning and deep learning. He has a master's in Embedded and Intelligent systems at Halmstad University and a bachelor's in Electronics and Communication Engineering from India.



Sushanth is an active researcher in the field of machine learning with a background in image processing, pattern recognition. He has a master's in Embedded and Intelligent systems at Halmstad University and a bachelor's in Electronics and Communication Engineering from India



PO Box 823, SE-301 18 Halmstad
Phone: +35 46 16 71 00
E-mail: registrator@hh.se
www.hh.se